

## Stabilized magnetic spin dimer entanglement using a genetic algorithm

Jin Wang

To cite this article: Jin Wang (2021): Stabilized magnetic spin dimer entanglement using a genetic algorithm, Journal of Modern Optics, DOI: [10.1080/09500340.2021.1998840](https://doi.org/10.1080/09500340.2021.1998840)

To link to this article: <https://doi.org/10.1080/09500340.2021.1998840>



Published online: 13 Nov 2021.



Submit your article to this journal [↗](#)



View related articles [↗](#)



View Crossmark data [↗](#)



# Stabilized magnetic spin dimer entanglement using a genetic algorithm

Jin Wang

Department of Natural Sciences, University of Michigan-Dearborn, Dearborn, MI, USA

## ABSTRACT

Genetic algorithm optimized time varying magnetic field functions for stabilizing and maximizing entanglement in a decoherence-free Heisenberg spin dimer are presented. The oscillation in entanglement in a decoherence free magnetic spin dimer is presented. The effect on the coherence and population terms in the density matrix due to the time-varying magnetic field functions is discussed and viewed using two dimensional time varying plots of entanglement and three-dimensional Bloch sphere diagrams. This work shows that it is possible to remove the natural oscillatory nature of decoherence free entanglement and maximize entanglement using time varying transient magnetic field stabilizing functions.

## ARTICLE HISTORY

Received 28 June 2021  
Accepted 22 October 2021

## KEYWORDS

Genetic algorithm;  
entanglement

## 1. Introduction

The quantum entanglement phenomenon is observed experimentally and mathematically as two or more quantum systems sharing the same wave function such that when measuring one system, the other system is affected instantaneously regardless of the distance. Quantum entanglement has been demonstrated to exist between quantum systems even at very large separations, for instance, distances such as between a satellite and the surface of earth [1]. Quantum entanglement is important to implement applications of quantum teleportation, quantum cryptography and quantum computation. Finding new ways to maximize and maintain the entanglement between two quantum systems is an active research area [2–4].

An interesting system for analysing entanglement is the behaviour of a Heisenberg spin dimer immersed in an external magnetic field. Entanglement in such systems has been studied for various spin chain models [5–8]. A time-invariant magnetic field of different magnitudes was able to change the oscillation frequency of entanglement in the Heisenberg spin dimer numerical model [7]. As will be shown, in this paper, it is possible to use a time-varying magnetic field to put a decoherence-free magnetic spin dimer into a constant nearly perfect entangled state. This paper uses simulation to show a decoherence-free magnetic spin dimer in a time-invariant magnetic field will naturally oscillate between zero and maximum entanglement. During the oscillation of the system when the system is in the unentangled state it cannot

be used for quantum computations. This paper analyses the system state difference between a time-invariant and a time-varying magnetic field stabilized spin dimer. To the author's knowledge, there is no analytical formula for finding the time-varying magnetic field function to stabilize a spin dimer. By using a genetic algorithm to find a time-varying magnetic field function, it can shed some light as to what the magnetic field solutions look like and how the system evolves into a stable entangled state.

## 2. The spin dimer system

In this work, a two qubit XY Heisenberg spin dimer with a static and time varying external magnetic field is considered. The system state evolves according to the equation of motion in Equation (1).

$$\frac{d\rho}{dt} = -i[H, \rho] \quad (1)$$

The density matrix  $\rho$  is a  $4 \times 4$  matrix in the form given in Equation (2). The diagonal terms of the matrix  $\rho$  represent the population and all sum to 1 which represents the total probability. The off diagonal terms represent coherence in the system.

$$\rho = \begin{pmatrix} \rho_{11} & \rho_{12} & \rho_{13} & \rho_{14} \\ \rho_{21} & \rho_{22} & \rho_{23} & \rho_{24} \\ \rho_{31} & \rho_{32} & \rho_{33} & \rho_{34} \\ \rho_{41} & \rho_{42} & \rho_{43} & \rho_{44} \end{pmatrix} \quad (2)$$

The Hamiltonian  $H$  of the spin dimer is given by Equation (3) [6].

$$H = B(t)(S_1^z + S_2^z) + J(S_1^+ S_2^- + S_1^- S_2^+) + Jr(S_1^+ S_2^+ + S_1^- S_2^-) \quad (3)$$

The raising and lowering operators for the spin system ( $S^\pm$ ) are defined according to:  $S_n^\pm = S_n^x \pm iS_n^y$ ,  $S_n^{(x,y,z)} = \frac{1}{2}\sigma_n^{(x,y,z)}$  with  $\sigma_n^{(x,y,z)}$  denoting the three Pauli spin matrices and  $n$  denoting the  $n$ th position on the spin chain. This Hamiltonian is described in terms of the parameters:  $J$ ,  $r$ , and  $B$ , where  $J = (J_x + J_y)/2$ , and  $r = (J_x - J_y)/(J_x + J_y)$ . The terms  $J_x$  and  $J_y$  denote the exchange interaction between two qubits in each dimension with positive values denoting anti-ferromagnetic interaction and negative values denoting ferromagnetic interaction. The coupling constant  $J$  and  $r$  play a role in entanglement as discussed in the literature [9].

The first term  $B(t)S_n^z$  shows the response of the system to an external time-varying magnetic field. The external magnetic field is taken to be directed along the  $z$ -axis, and is a function of time. The second and third terms describe the internal interactions of the system, which are governed by the coupling strength between the spin states ( $J$ ), and the asymmetry of this coupling ( $r$ ).

The concurrence measure is used to quantify the entanglement in this work [10].  $R$  is constructed from the system density matrix  $\rho$  in Equation (4). The concurrence  $C$  is defined by Equation (5) in which the  $\lambda_i$  represent the eigenvalues of the matrix  $R$ .

$$R = \rho(\sigma_y \otimes \sigma_y) \rho^* (\sigma_y \otimes \sigma_y) \quad (4)$$

$$C = \max(\sqrt{\lambda_1} - \sqrt{\lambda_2} - \sqrt{\lambda_3} - \sqrt{\lambda_4}, 0) \quad (5)$$

### 3. Genetic algorithm entanglement optimization

Since there is no cookbook method to find the time-varying magnetic field function to put the system into a stable entangled state, two general purpose approximation functions were considered. The first is to optimize the magnetic field intensity for each time point for the entire simulation, but this method creates an exponential number of parameters in the multidimensional optimization space for increasing time. The second and chosen method uses cubic spline interpolation since the control points only affect the nearest neighbours, and it reduces the number of parameters to optimize. To further reduce the number of parameters to optimize, only the first few time units of the simulation allow the magnetic field to vary. For the rest of the simulation after the initial time-varying period, the magnetic field is a constant  $a_0$ . One

other advantage of only varying the magnetic field at the beginning of the simulation is that in a practical application, the magnetic field would only need to be varied initially to put the spin dimer into an entangled state before using it to perform a quantum calculation. In addition to optimizing the control points for the cubic spline interpolation function for the magnetic field amplitude, the parameters  $J$ ,  $r$ , and  $a_0$  were optimized at the same time.

The genetic algorithm (GA) is a search algorithm inspired by the theory of evolution, and knowledge of how the genetic code is passed down to offspring [11]. The genetic algorithm in this paper did not use the concept of a 'generation' and simply replaces individuals in the population with roulette wheel selection as new individuals are created from the genetic operators. The shared fitness of a particular solution is proportional to the entanglement and inversely proportional to the Euclidean distance to the other solutions. Each individual consisted of all the parameters required to form a solution. The mutation operator modifies parameters by adding a Gaussian distributed random number. The crossover function is only allowed to cross over at parameter boundaries. A few additional operators were used such as gradient ascent, centre of mass, binary search, and swap. The gradient ascent operator attempts to move in the direction of the maximum increase in fitness based on two parents. The centre of mass operator uses a local population around each parent to calculate a set of parameters that would represent the centre of mass where the mass is the shared fitness. The binary search operator averages the parameters that lie between the two parents. The swap operation swaps the values of different parameters in the same individual. So, a swap might consist of swapping the values between parameter one and parameter ten. The simulation consisted of a population of 330, and 10,000 total number of fitness or entanglement evaluations.

### 4. Results

There are a number of results that were noteworthy from this investigation. The first is that the system entanglement from an initially constant magnetic field oscillates between maximum and minimum entanglement as shown in Figure 1. The genetic algorithm found an optimized constant magnetic field configuration, consisting of a magnetic field strength of amplitude  $a_0 = 0.0206$ , the coupling constant  $J = 1.3087$ , and the ratio  $r = 1.0735$ . In the figure, the excited and ground-state populations are shown. The total population is the sum of the ground  $\rho_{11}$  and excited  $\rho_{44}$  states. The populations oscillate with a constant amplitude sinusoidal pattern

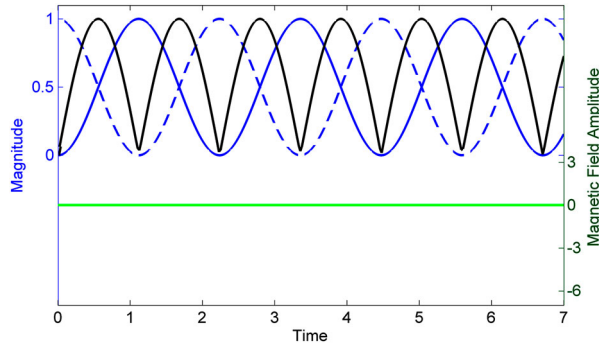


**Figure 1.** The excited state  $\rho_{11}$  is represented as a sinusoidal solid (blue) line while the ground state  $\rho_{44}$  is a dashed (blue) line. The entanglement is represented by the rectified sinusoidal solid (black) line. The magnetic field is a the bottom (green) solid line which is time-invariant. The horizontal axis represents the passage of time. The spin dimer system starts out initially in the ground state  $\rho_{44} = 1$ . The magnetic field is constant. The term  $\rho_{41}$  is the complex conjugate of  $\rho_{14}$  and is not plotted. The other terms of the density matrix are zero and do not vary with time.

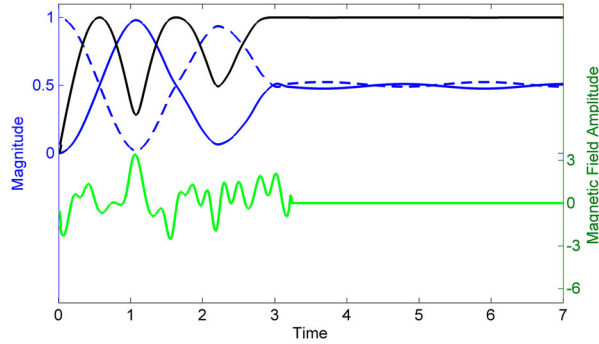


**Figure 2.** The same as Figure 1 except the bottom solid (green) line now varies according to the time-varying magnetic field from the first trial solution.

with the excited and ground state population 180-degree phase shift between them. The entanglement is maximized when the ground and excited-state populations are equal at 50%. This represents a superposition state where the two atomic states cannot be differentiated from each other. The entanglement goes to zero when either the ground or excited state populations are at a maximum. The  $\rho_{14}$  and  $\rho_{41}$  are the coherence terms that need to have a non-zero magnitude in order for the system to be entangled. A desirable situation would be if the entanglement was stable for a time-invariant magnetic field. This can be accomplished by manipulating the system to the desired state with a transient time-varying magnetic field as shown in Figures 2 and 3.

The magnetic field versus time function  $B(t)$  consists of two parts. The first is a time-varying initial 3.2-time units, and the second is a constant time independent field of magnitude  $a_0$  for the rest of the simulation time.

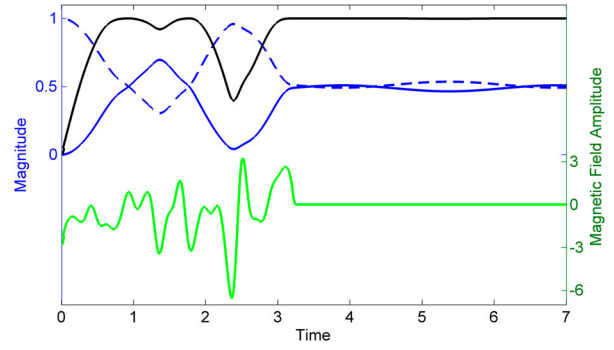


**Figure 3.** The same as Figure 1 except the bottom solid (green) line now varies according to the time varying magnetic field from the second trial solution.

The time-varying magnetic field functions are plotted in Figures 2 and 3. As shown in the figures, two different magnetic field functions lead to the same density matrix and stable entanglement. The time-varying magnetic field does not have an obvious relationship between the density matrix terms. In order to understand more about how the changing magnetic field causes the system to evolve into a stable entangled state, a three-dimensional plot of the coherence term  $\rho_{14}$  where the x dimension is the real and the y dimension is the imaginary part of  $\rho_{14}$ , and the z dimension represents time is displayed in Figures 4 and 5. Both the time-invariant and time-varying magnetic fields cause fluctuations in the imaginary part of  $\rho_{14}$ , but the real part for the time-invariant magnetic field only fluctuates around zero. During the two trials of time-varying magnetic field application, the real part changes from 0 to  $-0.5$ . The path taken by the  $\rho_{14}$  term is different in the trials, but end up in the same final state. Also, once the field goes to a constant value, the real part does not appear to fluctuate and the oscillations in the imaginary domain are nearly at zero amplitude. Furthermore, the spin dimer remains fully entangled with the same constant magnetic field that would otherwise exhibit oscillations in the entanglement without the initial changing magnetic field.

Another way to visualize the spin dimers during the application of the magnetic field function is to plot the evolution on the Bloch sphere. The results of two trials are shown in Figures 6 and 7. From this point of view, it is easy to see that when  $\rho_{14}$  is near the equator, the system exhibits entanglement. It is also clear that the system travels in a large loop from the ground to the excited state passing through the equator similar to a Rabi oscillation with a constant magnetic field. So, the system does not exhibit stable entanglement. However, when the dynamic magnetic field is applied, the system state

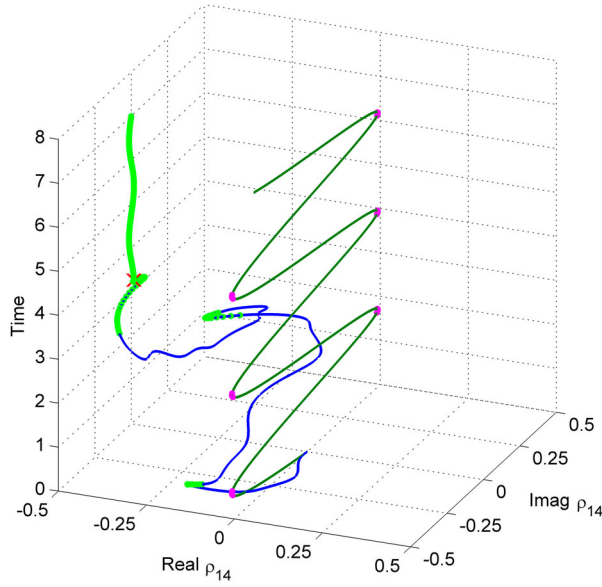


**Figure 4.** The real and imaginary parts of  $\rho_{14}$  are plotted against each other and as a function of time for an initial ground state. The sinusoidal (dark green) signal on the right where the real part of  $\rho_{14}$  is zero represents how the imaginary part of  $\rho_{14}$  in a constant magnetic field varies with time. The solid (blue) line starting at the bottom of the figure with zero real and imaginary components represents the irregular path  $\rho_{14}$  evolves during the time-varying magnetic field from trial 1 and then during a constant magnetic field after 3.2-time units. The highlighted (bright green) parts on the irregular (blue) line represent where entanglement is nearly one. The highlighted (purple) dots of the sinusoidal  $\rho_{14}$  evolution with a real part of zero represent where the entanglement is nearly one. The spin dimer state starts at the ground state, initially goes to the right then progresses to a real amplitude of  $-0.5$ . The B field as a function of time causes the system to evolve from the original ground state to a real part of  $-0.5$ .

changes to a small loop around  $X = -1$ , and exhibits stable entanglement.

## 5. Discussion and conclusion

This paper demonstrates using a genetic algorithm to find a time-varying magnetic field function to convert an unstable spin dimer system to exhibit stable entanglement. The analysis of the coherence term  $\rho_{14}$  during the transition from the unstable initial entanglement to the stable entanglement indicates the magnitude of the real part is important to maintain entanglement, and when it is near the equator of the Bloch sphere. The system evolves from an entanglement unstable orbit around the Bloch sphere near the poles to orbiting around the equator in a small loop. The entanglement is stable in the small loop since the density matrix  $\rho$  is always near the equator. Additionally, the constant magnetic field used to maintain the entangled state was less than 1% of the magnetic

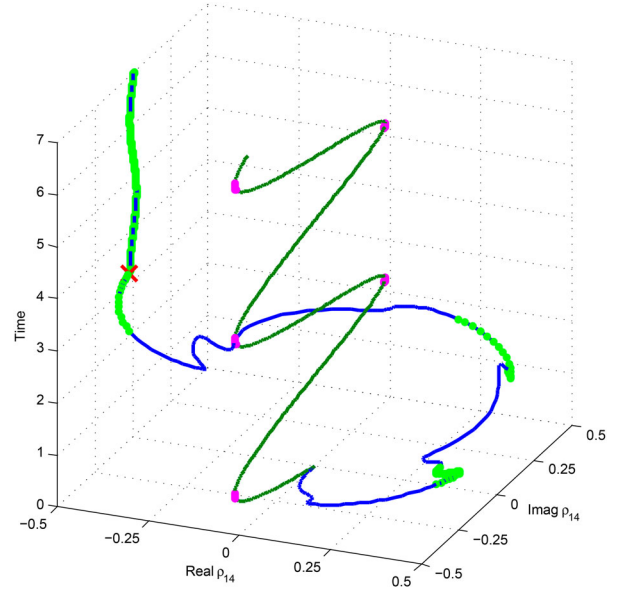


**Figure 5.** Same as Figure 4 except the time varying field is from trial solution 2. The start and end states are nearly identical, but the path to the final state is different.

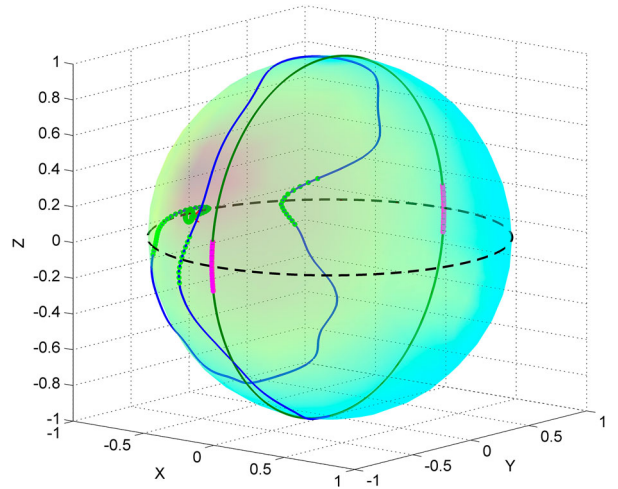


**Figure 6.** The Bloch Sphere representation of how the spin dimer state evolves for both a time-invariant and changing magnetic field for the first trial results. The starting state for both the constant and changing magnetic fields is the ground state at the bottom of the sphere. The solid (green) circle traversing the poles represents how the system oscillates between excited and ground states for a time invariant magnetic field. The highlighted (purple) markers near the equator represent where entanglement is maximized. The irregular (blue) line starting at the ground state (bottom) represents how the spin dimer evolves during the first trial time-varying magnetic field and then during a constant magnetic field. The highlighted (bright green) parts near the equator of the irregular line on represent where entanglement is nearly one. The cross (red) on the equator where the irregular line ends represents when the magnetic field is made constant. The small (green) circle where the irregular line ends near  $X$  equals  $-1$  represents the stabilized entangled state.



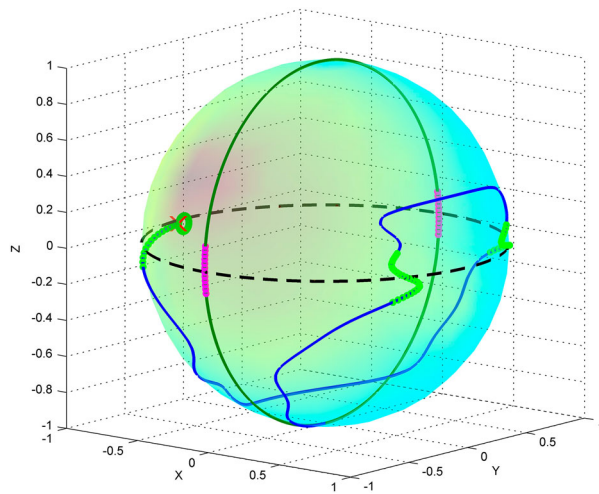


**Figure 7.** This is the second trial run result. See Figure 6 for the figure description.

field amplitude required to create the fully entangled state. The lower magnetic field required to maintain the entanglement has the benefit of lower maintenance cost and saves energy. In conclusion, this method of stabilizing maximum entanglement could be useful for quantum computing and higher efficiency with a lower energy requirement.

### Acknowledgments

The Author would like to thank the University of Michigan Office of the Vice President Research for support.

### Disclosure statement

No potential conflict of interest was reported by the author(s).

### References

- [1] Ren . Ground-to-satellite quantum teleportation. *Nature*. 2017;549:70–73.
- [2] Groisman B, Strelchuk S. Optimal amount of entanglement to distinguish quantum states instantaneously. *Phys Rev A*. 2015;92:052337. doi:10.1103/PhysRevA.92.052337
- [3] Rafiee M, Nourmandipour A, Mancini S. Optimal feed-back control of two-qubit entanglement in dissipative environments. *Phys Rev A*. 2016;94:012310. doi:10.1103/PhysRevA.94.012310
- [4] Sorelli G, Gessner M, Smerzi A, et al. Fast and optimal generation of entanglement in bosonic Josephson junctions. *Phys Rev A*. 2019;99:022329. doi:10.1103/PhysRevA.99.022329
- [5] Arnesen MC, Bose S, Vedral V. Natural thermal and magnetic entanglement in the 1D Heisenberg model. *Phys Rev Lett*. 2001;87:017901. doi:10.1103/PhysRevLett.87.017901
- [6] Lagmago Kamta G, Starace AF. Anisotropy and magnetic field effects on the entanglement of a two Qubit Heisenberg XY chain. *Phys Rev Lett*. 2002;88:107901. doi:10.1103/PhysRevLett.88.107901
- [7] Wang J, Landman M, Sutter T, et al. Entanglement evolution in a Heisenberg spin dimer. *IEEE Trans Magn*. 2019;55(12):1–3.
- [8] Wang X. Entanglement in the quantum Heisenberg XY model. *Phys Rev A*. 2001;64:012313. doi:10.1103/PhysRevA.64.012313
- [9] Wang J, Batelaan H, Podany J, et al. Entanglement evolution in the presence of decoherence. *J Phys B: At Mol Opt Phys*. 2006;39(21):4343–4353. doi:10.1088/0953-4075/39/21/001.
- [10] Hill S, Wootters WK. Entanglement of a pair of quantum bits. *Phys Rev Lett*. 1997;78:5022–5025. doi:10.1103/PhysRevLett.78.5022
- [11] Goldberg DE. Genetic algorithms in search, optimization, and machine learning. Addison-Wesley Publishing Company; 1989. (Artificial intelligence). Available from: [https://books.google.com/books?id=3\\_RQAAAAMAAJ](https://books.google.com/books?id=3_RQAAAAMAAJ)